Supplementary Information

Highly Transparent Ternary Bulk-Heterojunctions for Semi-transparent Organic Photovoltaics

*Hryhorii P. Parkhomenko[1§], Andrii I. Mostovyi[1§], Nora Schopp[2], Mykhailo M. Solovan[3], and Viktor V. Brus[1]**

[1] *Department of Physics, School of Sciences and Humanities, Nazarbayev University, Astana 010000, Kazakhstan*

[2] *First Solar Inc., 28101 Cedar Park Blvd, Perrysburg, Ohio 43551, United States*

[3] *Faculty of Physics, Adam Mickiewicz University, Poznan 61-614, Poland*

Corresponding Author

Viktor V. Brus Email: vvbrus@gmail.com; viktor.brus@nu.edu.kz

[§] *These authors contributed equally*

Table S1. AVT of BHJ layers reported in the literature.

Active layer	Thickness [nm]	AVT [%] of active layer	Reference
PCE10:PTAA:COTIC-4F	**76**	**82**	**This work**
PCE10:SiOTIC-4F	**79**	**72**	**This work**
PCE10:PTAA:SiOTIC-4F	**80**	**78**	**This work**
D18:N3	100	53	[1]
D18-Cl:Y6-1O	-	68	[2]
PM6:Y6	60	57.6	[3]
P1:$PC_{71}BM$	70	63	[4]
PTB7-Th:ITVfIC	100	59	[5]
66-PTB:IEICO-4F	-	70	[6]
PTB7-Th : IEICO-4F	100	60	[7]
	92	64	
PCE10:COTIC-4F	83	70	[8]
	78	77	

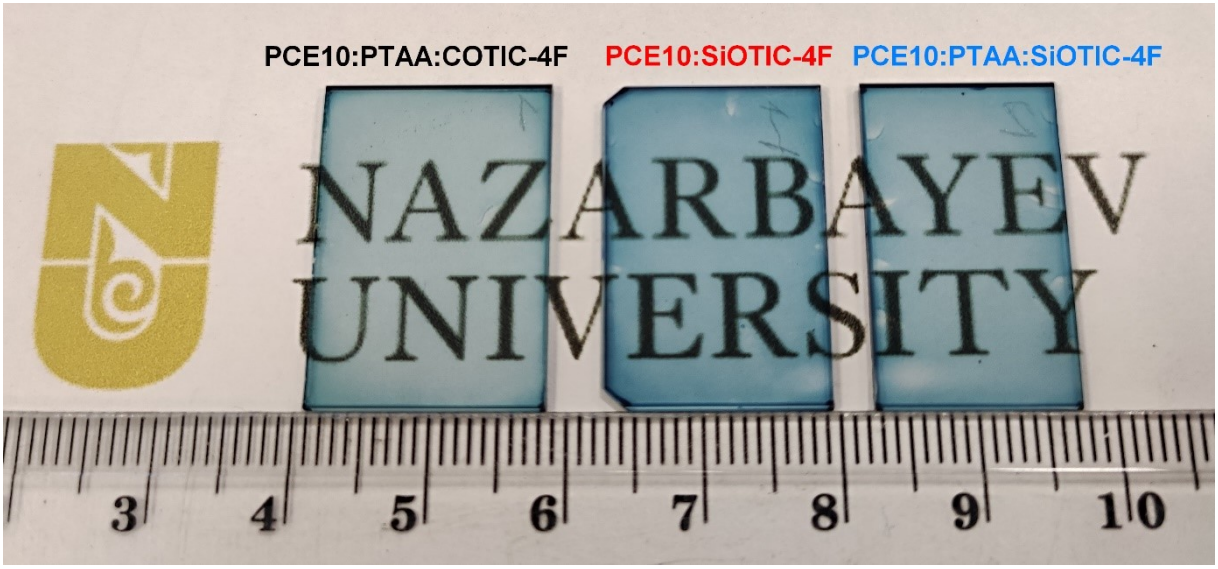

Fig. S1. Photo image of BHJ layers on a neutral paper background.

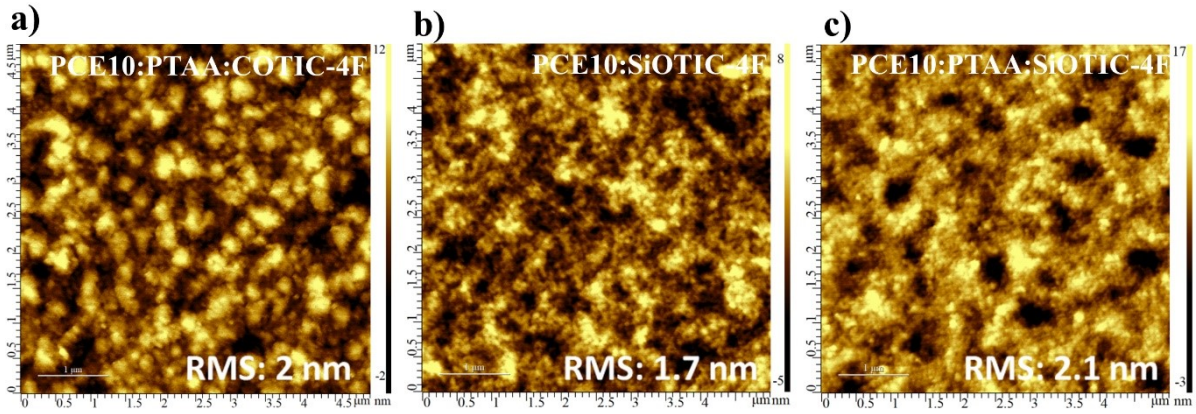

Fig. S2. AFM images of PCE10:PTAA:COTIC-4F (a), PCE10:SiOTIC-4F (b), and PCE10:PTAA:SiOTIC-4F (c) thin films.

Refractive index *n* and extinction coefficient *k*.

The optical constants were determined from the measured transmittance and reflectance spectra as described below.

If the condition $n^2 >> k^2$ is fulfilled and there is no interference, the absorption coefficient $\alpha(\lambda)$ and the refractive index $n(\lambda)$ of the OPV thin films can be calculated by the equations (S1) and (S2), respectively [9,10]:

$$\alpha = \frac{1}{d}\ln\left[\frac{(1-R)^2}{2T} + \sqrt{\frac{(1-R)^4}{4T^2} + R^2}\right]. \quad \text{(S1)}$$

$$n = \frac{1+\sqrt{R}}{1-\sqrt{R}}. \quad \text{(S2)}$$

The extinction coefficient can readily be found using the relation $k(\lambda) = \lambda\alpha(\lambda)/4\pi$.

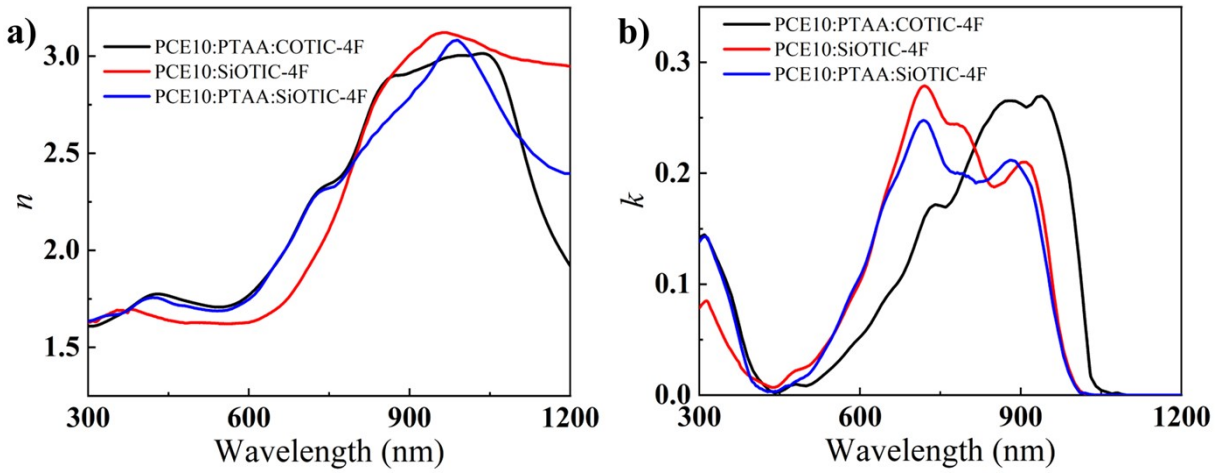

Fig. S3. Calculated (a) *n* and (b) *k* values of different BHJ layers based on transmittance and reflectance spectra.

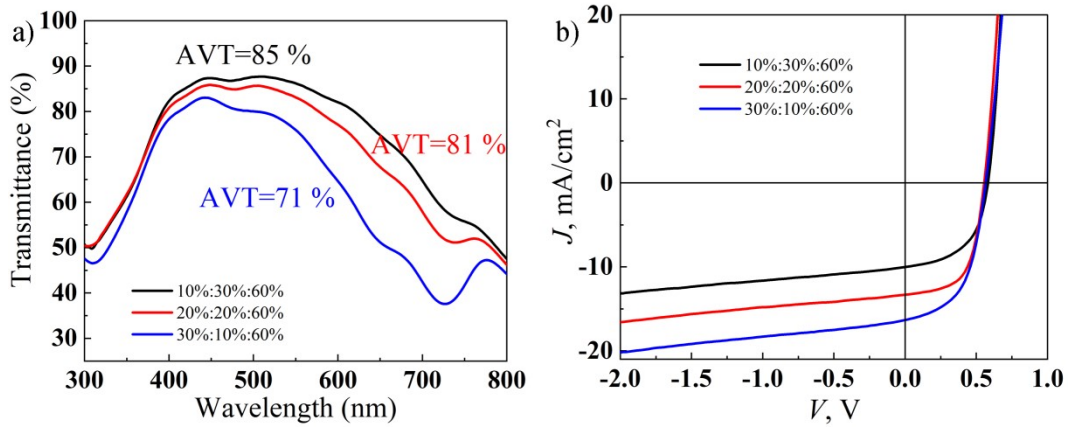

Figure S4. a) Transmittance spectra of the PCE10:PTAA:COTIC-4F blends with the different content of PCE10 and PTAA donors. b) *J-V* curves of the studied opaque OSCs with PCE10:PTAA:COTIC-4F active layers.

Table S2. Photovoltaic parameters of opaque OSCs with PCE10:PTAA:COTIC-4F blends with different PCE10 and PTAA donor content.

Ratio of PCE10:PTAA:COTIC-4F	J_{sc} [mA cm^{-2}]	V_{OC} [V]	FF [%]	PCE [%]	AVT [%] of the active layer
10%:30%:60%	10.02	0.58	51.3	2.99	85
20%:20%:60%	13.32	0.56	60.4	4.41	81
30%:10%:60%	16.48	0.56	51.9	4.79	71

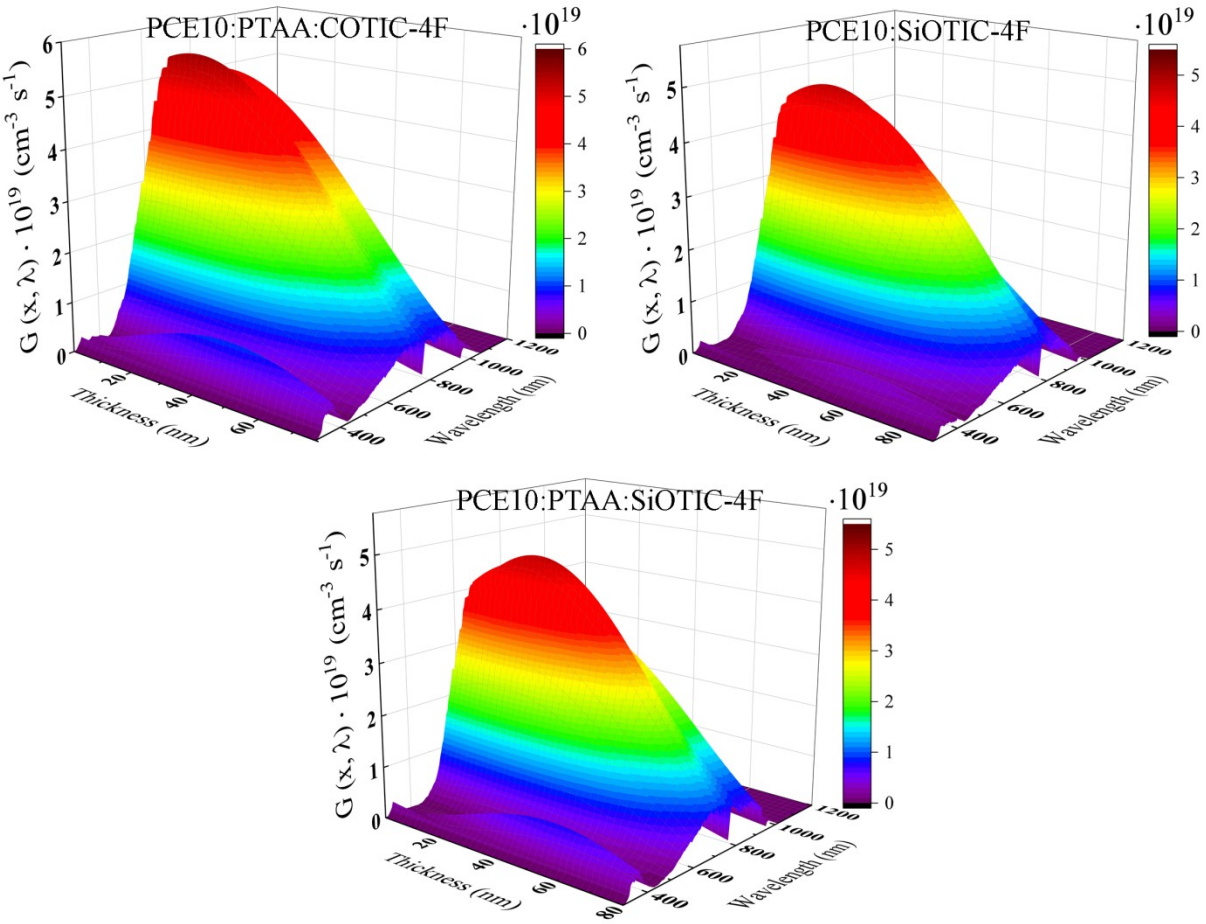

Fig. S5. Generation rates *G(x, λ)*, depending on the wavelength and position in the active layer, for AM 1.5 illumination.

Recombination Current Density

Fig. S5 shows the experimentally measured recombination current density (J_{rec}), determined using the equation:

$$J_{rec} = J_{ph,s} - J_{ph}, \tag{S3}$$

where $J_{ph,s}$ is the saturated photocurrent density at a reverse bias (-2 V). $J_{ph} = J_{Light} - J_{dark}$ is the photocurrent density.

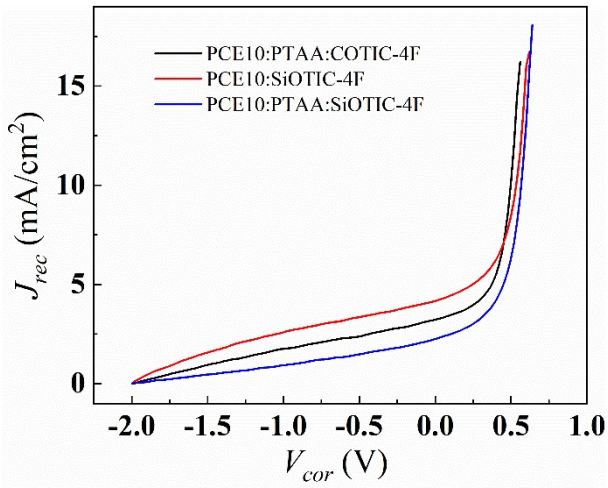

Fig. S6. Calculated J_{rec} for the OSCs under 1 sun illumination.

The total J_{rec} can be represented as the sum of individual recombination currents originating from different recombination mechanisms:

$$J_{rec,sum} = J_{r,bm} + J_{r,bt} + J_{r,st} \tag{S4}$$

where $J_{r,bm}$ is the bimolecular recombination current density, $J_{r,bt}$ is the recombination current density via bulk trap states, and $J_{r,st}$ is the recombination of current density via surface trap states. Each of these terms can be represented as follows: [11,12]

$$J_{r,bm} = \frac{q^2 L}{\varepsilon_r \varepsilon_o} \xi \mu_{eff} n^2, \tag{S5}$$

$$J_{r,bt} = \frac{q^2 L}{\varepsilon_r \varepsilon_o} \mu_{eff} N_{t,bulk} n, \tag{S6}$$

$$J_{r,st} = \frac{q^2 \quad \mu_{eff} N_{t,surf}\, n}{\varepsilon_r \varepsilon_o \; exp\left(\frac{q(V_{bi} - V)}{kT}\right)}, \tag{S7}$$

where ξ is the reduction factor (also known as Langevin prefactor), $N_{t,bulk}$ is the density of traps states in the bulk, $N_{t,surf}$ is the density of surface trap states, $\varepsilon_r = C_g L / \varepsilon_r A$, is the dielectric constant of the BHJ layer, ε_0 is the vacuum permittivity, L is the thickness of the BHJ layer, A

is the area of the device (0.1 cm^2), C_g is the frequency-independent capacitance of the BHJ layer measured at a large reverse bias (-2 V), and μ_{eff} is the effective mobility [11] (see Fig. S8).

Charge carrier concentration:

Impedance spectroscopy was utilized to measure corrected capacitance C_{cor}.

$$C_{cor} = -\frac{1}{\omega}\left[\frac{Z'' - \omega L}{(Z' - R_s)^2 + (Z'' - \omega L)^2}\right] \tag{S8}$$

The difference between barrier capacitance at low frequencies under light and dark conditions provides chemical capacitance $C_b = C_{cor.light} - C_{cor.dark}$, here $C_{cor.light}$ and $C_{cor.dark}$ is corrected capacitance at low frequencies under light and dark conditions, respectively (see Fig. S6).

The charge carrier density at different applying voltages can be calculated with Equation S9 and shown in Fig. S7.

$$n(V) = n_{sat} + \frac{1}{qAd}\int_{V_{sat}}^{V} C_b dV \tag{S9}$$

$$n_{sat} = \frac{1}{qAd} C_{sat}(V_0 - V_{sat}) \tag{S10}$$

where A is the solar cell area, d is the thickness, V_{sat} is the reverse bias where the photocurrent saturates (-0.5 V), and n_{sat} is the charge carrier density at the saturation voltage V_{sat}. The C_{sat} is the difference in capacitance of the PSC under light and dark at V_{sat}. Similarly, V_0 is the forward bias at which the photocurrent becomes zero.

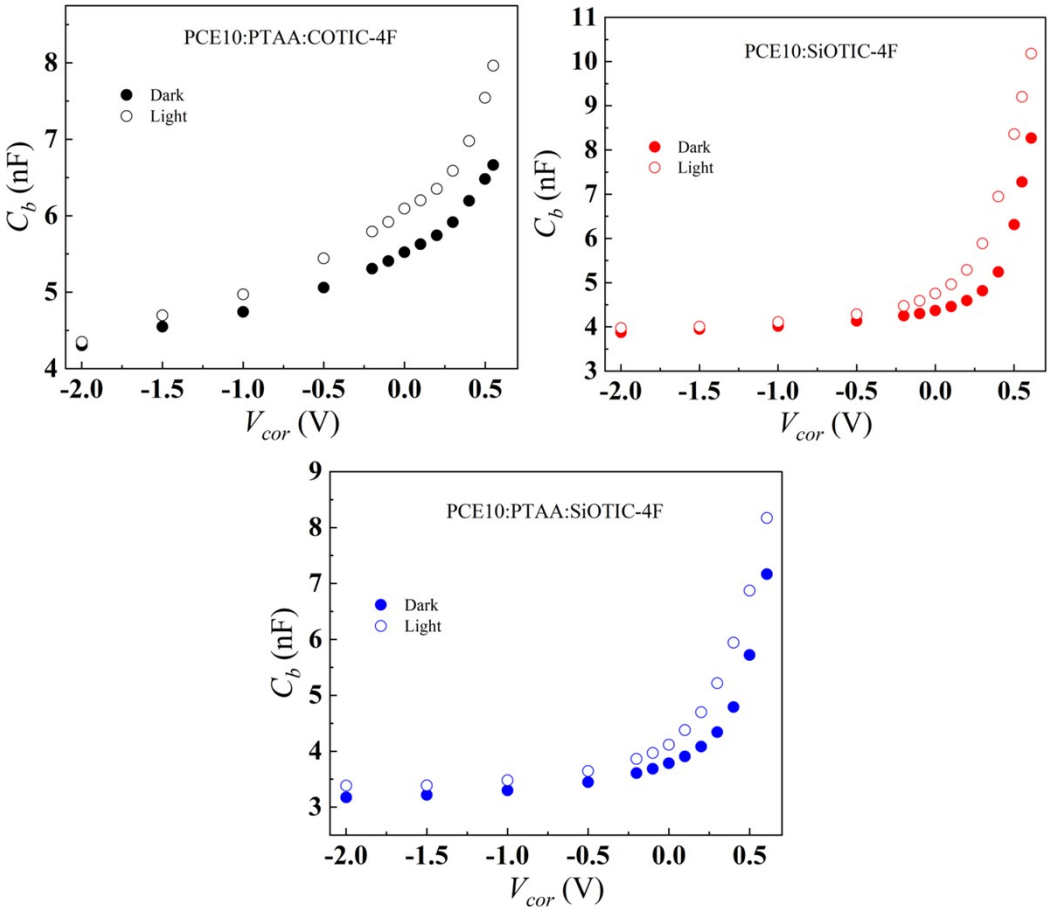

Fig. S7. The voltage-dependent capacitance of opaque OSCs.

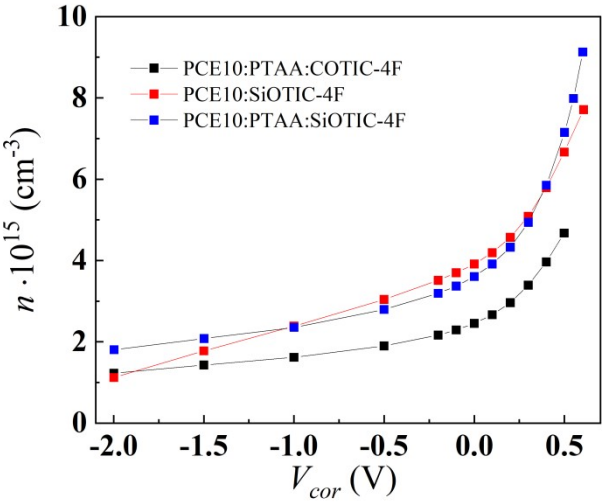

Fig. S8. Carrier concertations at different applied voltages.

Effective Mobility

The effective mobility (μ_{eff}) as a function of voltage (V) was calculated using the following equation [11,13]:

$$\mu_{eff}(n, V_{cor}) = \frac{J(V_{cor})L}{2qn(V_{cor})[V_{cor} - V_{OC}]} \quad \text{(S11)}$$

where V_{cor} is the corrected voltage, J is the current density, q is the elementary charge, L is the active layer thickness, and n is the charge carrier density.

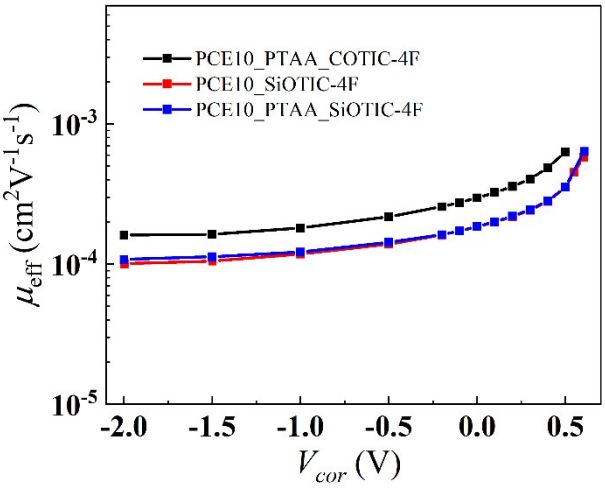

Fig. S9. Voltage dependence of effective mobility μ_{eff}.

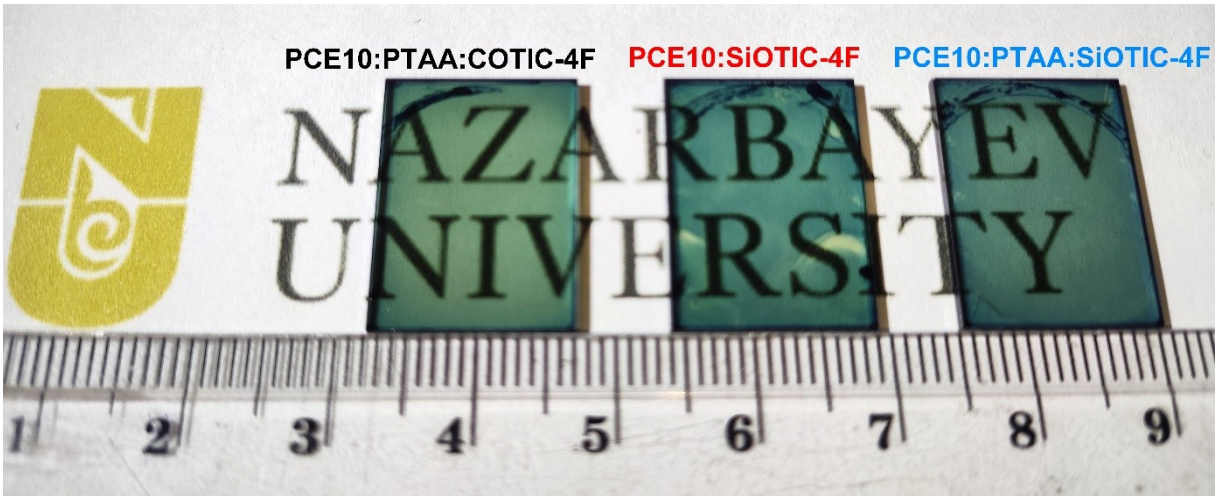

Fig. S10. Photo image of ST-OSCs on a neutral paper background.

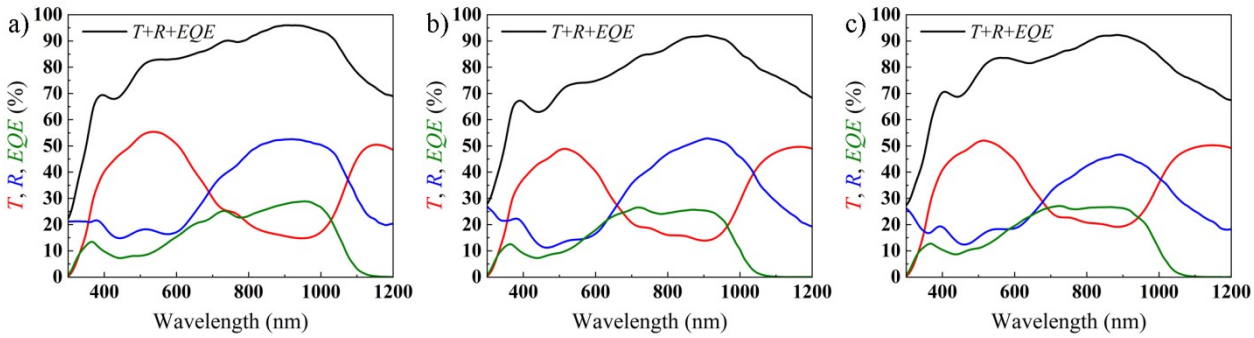

Figure S11. Photon balance: a) PCE10:PTAA:COTIC-4F active layer; b) PCE10:SiOTIC-4F active layer; c) PCE10:PTAA:SiOTIC-4F active layer.

Table S3. AVT and LUE reported in the literature.

Active layer	PCE [%]	AVT [%]	LUE [%]	Reference
PCE10:PTAA:COTIC-4F	**3.16**	**52.6**	**1.66**	**This work**
PCE10:SiOTIC-4F	**3.27**	**44.2**	**1.44**	**This work**
PCE10:PTAA:SiOTIC-4F	**3.64**	**48.2**	**1.75**	**This work**
D18:N3	12.7	22.49	2.9	[1]
D18-Cl:Y6-1O	12.94	20.2	2.63	[2]
PM6:Y6	12.37	18.6	2.3	[3]
PTB7-Th:ITVfIC	7.05	35	2.46	[5]
66-PTB:IEICO-4F	5.38	38.66	2.13	[6]
PTB7-Th : IEICO-4F	9.06	27.1	2.45	[7]
PCE10:COTIC-4F	3.3	41.9	1.38	[8]
	2.9	47.1	1.36	
	1.7	48.9	0.83	
PDTIDTBT:$PCB_{60}M$	4.75	55	2.61	[14]
PCDTBT:$PC_{71}BM$	3.9	34	1.33	[15]
PIDT-PhanQ:$PC_{71}BM$	5.1	24.4	1.24	
PTB7-Th:$PC_{71}BM$	6	30	1.8	
PBDTT-DPP:PCBM	4	55	2.2	
PBDTTPD:$PC_{70}BM$	4.3	34	1.46	[16]
PTB7-Th:$PC_{71}BM$	5.01	50.3	2.52	[17]
PBDTTT-C:Cy7-T: $PC_{70}BM$	3	51	1.53	[18]
P3TH:$PC_{61}BM$	1.97	42	0.83	[19]
P3HT:$PC_{60}BM$	2.4	70	1.68	[20]
PCDTBT:$PC_{71}BM$	1.9	40	0.76	[21]
PTB7:$PC_{71}BM$	3.75	35	1.31	[22]
PTB7:$PC_{71}BM$	4.2	40	1.68	[23]
J71:PTB7-Th:IHIC (0.4:0.6:1)	8.93	24.4	2.17	[24]
PTB7-Th:$PC_{71}BM$	9.36	14.31	1.34	[25]
PTB7:$PC_{71}BM$	5.6	30	1.68	[26]

PTB7-Th:IEICO-4F	11	30	3.3	[27]
PTB7-Th:BT-CIC:TT-FIC (1:1.25:0.5)	8.1	25.6	2.07	[28]
PBT1-C-2Cl:Y6	8.24	44.2	3.64	[29]
PCE10-2F:PM6:Y6	12.25	36.57	4.48	[30]
PM6:BTP-eC9:L8-BO	12.6	44.3	5.6	[31]

Reference:

1 C. Xu, K. Jin, Z. Xiao, Z. Zhao, X. Ma, X. Wang, J. Li, W. Xu, S. Zhang, L. Ding and F. Zhang, *Advanced Functional Materials*, 2021, **31**, 2107934.
2 Z. Hu, J. Wang, X. Ma, J. Gao, C. Xu, X. Wang, X. Zhang, Z. Wang and F. Zhang, *J. Mater. Chem. A*, 2021, **9**, 6797–6804.
3 Z. Hu, Z. Wang, Q. An and F. Zhang, *Science Bulletin*, 2020, **65**, 131–137.
4 H. Yin, J. K. W. Ho, V. Piradi, S. Chen, X. Zhu and S. K. So, *Small Methods*, 2020, **4**, 2000136.
5 H. Huang, X. Li, L. Zhong, B. Qiu, Y. Yang, Z.-G. Zhang, Z. Zhang and Y. Li, *J. Mater. Chem. A*, 2018, **6**, 4670–4677.
6 Q. Wei, Y. Zhang, T. Shan and H. Zhong, *J. Mater. Chem. C*, 2022, **10**, 5887–5895.
7 Z. Hu, Z. Wang and F. Zhang, *J. Mater. Chem. A*, 2019, **7**, 7025–7032.
8 N. Schopp, G. Akhtanova, P. Panoy, A. Arbuz, S. Chae, A. Yi, H. J. Kim, V. Promarak, T.-Q. Nguyen and V. V. Brus, *Advanced Materials*, 2022, **34**, 2203796.
9 Iu. I. Ukhanov, *Moscow Izdatel Nauka*.
10 M. Solovan, V. Brus, E. Maistruk and P. Maryanchuk, *Inorganic Materials*, 2014, **50**, 40–45.
11 J. Vollbrecht, V. V. Brus, S.-J. Ko, J. Lee, A. Karki, D. X. Cao, K. Cho, G. C. Bazan and T.-Q. Nguyen, *Advanced Energy Materials*, 2019, **9**, 1901438.
12 M. Kuik, L. J. A. Koster, G. A. H. Wetzelaer and P. W. M. Blom, *Phys. Rev. Lett.*, 2011, **107**, 256805.
13 S. Albrecht, J. R. Tumbleston, S. Janietz, I. Dumsch, S. Allard, U. Scherf, H. Ade and D. Neher, *J. Phys. Chem. Lett.*, 2014, **5**, 1131–1138.
14 M. M. Tavakoli, R. Po, G. Bianchi, A. Cominetti, C. Carbonera, N. Camaioni, F. Tinti and J. Kong, *Proceedings of the National Academy of Sciences*, 2019, **116**, 22037–22043.
15 Z. Hu, J. Wang, X. Ma, J. Gao, C. Xu, K. Yang, Z. Wang, J. Zhang and F. Zhang, *Nano Energy*, 2020, **78**, 105376.
16 Z. M. Beiley, M. G. Christoforo, P. Gratia, A. R. Bowring, P. Eberspacher, G. Y. Margulis, C. Cabanetos, P. M. Beaujuge, A. Salleo and M. D. McGehee, *Advanced Materials*, 2013, **25**, 7020–7026.
17 G. Ji, Y. Wang, Q. Luo, K. Han, M. Xie, L. Zhang, N. Wu, J. Lin, S. Xiao, Y.-Q. Li, L.-Q. Luo and C.-Q. Ma, *ACS Appl. Mater. Interfaces*, 2018, **10**, 943–954.
18 M. Makha, P. Testa, S. B. Anantharaman, J. Heier, S. Jenatsch, N. Leclaire, J.-N. Tisserant, A. C. Véron, L. Wang, F. Nüesch and R. Hany, *Science and Technology of Advanced Materials*, 2017, **18**, 68–75.
19 D. Zhang, R. Wang, M. Wen, D. Weng, X. Cui, J. Sun, H. Li and Y. Lu, *J. Am. Chem. Soc.*, 2012, **134**, 14283–14286.
20 Y. Zhou, H. Cheun, S. Choi, C. Fuentes-Hernandez and B. Kippelen, *Organic Electronics*, 2011, **12**, 827–831.
21 J. Czolk, A. Puetz, D. Kutsarov, M. Reinhard, U. Lemmer and A. Colsmann, *Advanced Energy Materials*, 2013, **3**, 386–390.
22 X. Fan, B. Xu, N. Wang, J. Wang, S. Liu, H. Wang and F. Yan, *Advanced Electronic Materials*, 2017, **3**, 1600471.
23 Z. Liu, P. You, S. Liu and F. Yan, *ACS Nano*, 2015, **9**, 12026–12034.

24 J. Zhang, G. Xu, F. Tao, G. Zeng, M. Zhang, Y. (Michael) Yang, Y. Li and Y. Li, *Advanced Materials*, 2019, **31**, 1807159.
25 P. Shen, M. Yao, J. Liu, Y. Long, W. Guo and L. Shen, *J. Mater. Chem. A*, 2019, **7**, 4102–4109.
26 R. Betancur, P. Romero-Gomez, A. Martinez-Otero, X. Elias, M. Maymó and J. Martorell, *Nature Photon*, 2013, **7**, 995–1000.
27 R. Xia, C. J. Brabec, H.-L. Yip and Y. Cao, *Joule*, 2019, **3**, 2241–2254.
28 Y. Li, C. Ji, Y. Qu, X. Huang, S. Hou, C.-Z. Li, L.-S. Liao, L. J. Guo and S. R. Forrest, *Advanced Materials*, 2019, **31**, 1903173.
29 Y. Xie, Y. Cai, L. Zhu, R. Xia, L. Ye, X. Feng, H.-L. Yip, F. Liu, G. Lu, S. Tan and Y. Sun, *Advanced Functional Materials*, 2020, **30**, 2002181.
30 L. Zhao, X. Huang, Y. Wang, S. Young Jeong, B. Huang, J. Deng, J. Liu, Y. Cheng, H. Young Woo, F. Wu, L. Chen and L. Chen, *Chemical Engineering Journal*, 2023, **451**, 139081.
31 Y.-F. Zhang, W.-S. Chen, J.-D. Chen, H. Ren, H.-Y. Hou, S. Tian, H.-R. Ge, H.-H. Ling, J.-L. Zhang, H. Mao, J.-X. Tang and Y.-Q. Li, *Advanced Energy Materials*, **n/a**, 2400970.